Agricultural and Forest Meteorology 253–254 (2018) 247–260

Contents lists available at ScienceDirect

Agricultural and Forest Meteorology

journal homepage: www.elsevier.com/locate/agrformet

Mapping forest canopy nitrogen content by inversion of coupled leaf-canopy radiative transfer models from airborne hyperspectral imagery

Zhihui Wang[a,b,*], Andrew K. Skidmore[a], Roshanak Darvishzadeh[a], Tiejun Wang[a]

[a] Faculty of Geo-Information Science and Earth Observation (ITC), University of Twente, P.O. Box 217, 7500 AE Enschede, The Netherlands
[b] School of Mathematical and Geospatial Sciences, RMIT University, GPO Box 2476, Melbourne, Victoria 3001, Australia

ARTICLE INFO

Keywords:
Leaf and canopy nitrogen
Forest
Radiative transfer model
Model inversion
PROSPECT
INFORM
Hyperspectral remote sensing

ABSTRACT

Foliar nitrogen is a critical factor in leaf physiological processes, plant growth, and ecosystem functioning, which has been proposed as one of the essential biodiversity variables. Nitrogen has been quantified by a number of empirical approaches using hyperspectral data, but the retrieval of nitrogen through a physically based approach remains a challenge. A recent study by Wang et al. (2015a) has revealed that leaf protein can be successfully estimated from fresh leaf spectra using a revised leaf radiative transfer model PROPECT-5 which incorporated the effects of leaf protein and cellulose + lignin on leaf reflectance and transmittance. This provides a potential approach of estimating nitrogen using radiative transfer models given the correlation between protein and nitrogen. However, such a revised leaf model has not been tested for the estimation of leaf nitrogen at the canopy level. In this study, a canopy reflectance model INFORM, coupled with the revised PROSPECT-5 model, was used to retrieve leaf and canopy nitrogen content in a mixed temperate forest using the wavelengths of 800–2500 nm from airborne hyperspectral imagery. Ecological criteria were applied to the parameterization of the model to reduce unrealistic combinations of input parameters. Global sensitivity analysis showed that leaf protein played a small but distinct role in driving the variation of canopy reflectance in the INFORM model. More accurate estimation was obtained for canopy nitrogen content (R^2 = 0.64, RMSE = 1.90, NRMSE = 0.18) than leaf nitrogen content (R^2 = 0.46, RMSE = 3.79e-05, NRMSE = 0.19). Moreover, inversion techniques, particularly regularized look-up tables, further improved the estimation accuracies compared to the original tables. Our results indicate that leaf and canopy nitrogen content can be retrieved successfully at the canopy level by inversion of INFORM. Both the direct and indirect effects of nitrogen on canopy reflectance are important for nitrogen estimation. The maps of leaf and canopy nitrogen content are the first to be generated using inversion of coupled leaf-canopy models, and the spatial variation of foliar nitrogen appears to be reasonable and consistent with ecological knowledge.

1. Introduction

Leaf nitrogen is an important parameter related to photosynthesis and net primary production (Evans, 1989; Field and Mooney, 1986; Reich, 2012), which mainly exists in chlorophylls and proteins in the leaf cells (Elvidge, 1990; Evans, 1983). Estimation of leaf nitrogen improves our understanding of terrestrial ecosystem carbon dynamics and climate models (Lamarque et al., 2005; Morford et al., 2011; Ollinger et al., 2008). As one of the essential biodiversity variables, foliar nitrogen can be used to assess biodiversity and ecosystem services (Pereira et al., 2013; Skidmore et al., 2015). Accurate retrieval of leaf nitrogen could therefore enhance ecosystem process models that describe ecosystem functioning, since nitrogen is an important input parameter of these models (Zaehle et al., 2014; Zhang et al., 2013).

Although leaf nitrogen is a small constituent of leaf dry weight (0.2%–6.4%) (Wright et al., 2004), it has been quantified from leaf and canopy spectra on the basis that the nitrogen absorption features can be detected by the narrow-band of continuous information from hyperspectral remote sensing (Cho, 2007). A number of factors confound the retrieval of leaf nitrogen from leaf and canopy spectra. Leaf water is one of the main obstacles for estimating leaf nitrogen using the fresh leaf spectra, because the strong absorption of water masks the spectral features of nitrogenous biochemicals in the short-wave near infrared (SWIR) spectral region (Fourty and Baret, 1998; Kokaly and Clark, 1999). Other constituents in leaves, such as cellulose, lignin and starch, also overlap with the absorption features of nitrogen in SWIR regions (Curran, 1989), which further increases the difficulty of retrieving nitrogen content. When estimating leaf nitrogen from the canopy spectra,

* Corresponding author at: Department of Forest and Wildlife Ecology, University of Wisconsin-Madison, 1630 Linden Drive, Madison, WI 53706, USA.
E-mail address: zwang896@wisc.edu (Z. Wang).

https://doi.org/10.1016/j.agrformet.2018.02.010
Received 20 August 2017; Received in revised form 19 January 2018; Accepted 12 February 2018
Available online 28 February 2018
0168-1923/

factors such as canopy structure, illumination/viewing geometry, and the background can further decrease our ability to detect nitrogen (Asner, 1998; Knyazikhin et al., 2013; Yoder and Pettigrew-Crosby, 1995; Zarco-Tejada et al., 2001).

Different approaches have been applied to improve leaf nitrogen estimation by enhancing the absorption features of nitrogen and reducing the influence of other factors on canopy reflectance. The approaches include spectral transformation such as using first/second derivatives and log transformation of reflectance (Coops et al., 2003; Yoder and Pettigrew-Crosby, 1995), continuum removal (Huang et al., 2004; Kokaly and Clark, 1999), water removal (Ramoelo et al., 2011; Schlerf et al., 2010), and wavelet analysis (Ferwerda and Jones, 2006). Empirical approaches such as vegetation indices (Serrano et al., 2002; Wang et al., 2016), stepwise multiple linear regression (Kokaly and Clark, 1999), partial least squares regression (Lepine et al., 2016; Martin et al. 2008), neural networks (Skidmore et al., 2010), and support vector regression (Axelsson et al., 2013) have been used to establish relationships between spectral data and nitrogen. However, such empirical relationships have been site-, sensor-, date- or species-specific. In addition, the selected wavelengths that are sensitive to nitrogen in different studies are not always consistent, and often deviate from the absorption bands of nitrogen (Curran et al., 2001; Huang et al., 2004; Kokaly and Clark, 1999). The important wavelengths for nitrogen estimation have been identified in the red-edge region, the near-infrared region, and short-wave infrared regions (Kokaly et al., 2009; Homolova et al., 2013). The accurate retrieval of nitrogen can be attributed to the association of nitrogen with chlorophyll, dry matter, water and canopy structure (Knyazikhin et al., 2013; Homolova et al., 2013; Wang et al., 2015b). However, the protein absorption features (mainly in the 800–2500 nm region) have not been successfully used to directly derive nitrogen at a reasonable level of accuracy.

Radiative transfer models (RTMs) offer a conceptual superiority to empirical approaches with respect to transferability and robustness (Darvishzadeh et al., 2011; Jacquemoud and Baret, 1990; Schlerf and Atzberger, 2006). In these models, the transfer and interactions of electromagnetic radiation inside the canopies are described based on physical laws (Verhoef, 1984). Depending on the model type, i.e. leaf or canopy, the absorbing and scattering processes of radiation are incorporated using a range of leaf, canopy and external parameters (Jacquemoud and Baret, 1990; Verhoef, 1984). It was considered impossible to retrieve leaf nitrogen from fresh leaves using leaf RTMs (Jacquemoud et al., 1996). However, a recent study showed that leaf protein can be estimated through the leaf optical properties model PROSPECT-5 (Feret et al., 2008), which was revised to incorporate both protein as well as cellulose + lignin compounds as a replacement for the dry matter (Wang et al., 2015a). Protein is determined based on the presence of nitrogen, with the Kjeldahl (or similar) method being almost universally applied to determine nitrogen, and a conversion factor of 6.25 is used to convert nitrogen to protein for both the animal feed and food materials industries (Barton, 1987; AOAC, 1990; Jacquemoud et al., 1996). This protein-nitrogen relationship provides the possibility of direct estimation of nitrogen using radiative transfer models. However, the feasibility of retrieving leaf nitrogen at the canopy level has not yet been assessed through coupling this revised leaf model with a canopy reflectance model.

The canopy reflectance model provides a means of understanding the covariance of leaf and canopy effects in canopy reflectance (Baret et al., 1994; Jacquemoud et al., 2000). There are generally four categories of canopy reflectance models: (1) 1D turbid medium model such as SAILH (Verhoef, 1984); (2) geometrical models such as Li–Strahler GO model (Li and Strahler, 1985); (3) Monte Carlo ray tracing models such as DART (Gastellu-Etchegorry et al., 1996); and (4) hybrid models such as GeoSail (Huemmrich, 2001). To select a proper canopy reflectance model, two factors should be considered (Atzberger, 2000; Pinty et al., 2004). The first factor is the realism of simulations with regard to the canopy architecture description, and the second is the invertibility of the model associated with a limited number of input variables. However, a model with more realistic simulations often leads to more complicated inversion, thus a compromise needs to be sought. The hybrid models benefit from a combination of 1D turbid medium and geometrical models (GO), which means they are closer to reality and easier to invert. The invertible forest reflectance model INFORM (Atzberger, 2000) is an example of a hybrid model that has been successful in retrieving vegetation parameters (Ali et al., 2016a; Schlerf and Atzberger, 2006, 2012; Yuan et al., 2015). As a hybrid model, INFORM could therefore offer a compromise between the realism of simulating the canopy and invertibility. We adopted the INFORM model for this study.

This study aimed (1) to assess if leaf and canopy nitrogen content could be retrieved from canopy spectra using the wavelengths of 800–2500 nm by inverting coupled leaf-canopy radiative transfer models; (2) to investigate if regulation techniques such as using prior information, spectral subsets and ecological constraints could improve the estimation accuracies; and (3) to map the spatial variation of leaf and canopy nitrogen content in a mixed temperate forest from airborne hyperspectral imagery.

2. Materials and methods

2.1. Study area and field data

2.1.1. Study area

The study area is located in the southern part of the Bavarian Forest National Park (49° 3′ 19″ N, 13° 12′ 9″ E), Germany (Fig. 1). The park has a total area of 24,218 ha. The geology is dominated by gneiss and granite, and the soils weathered from these parent materials are naturally acid and low in nutrients. The main soil types are brown soils, loose brown soils, and podsol brown soils. The park's elevation ranges from 600 m to 1453 m. The climate is temperate with a total annual precipitation between 1200 mm and 1800 mm and a mean annual temperature of 5.1 °C in the valleys, 5.8 °C on hillsides, and 3.8 °C in the higher montane zones (Heurich et al., 2010). The dominant forest species are Norway spruce (*Picea abies*) (67%) and European beech (*Fagus sylvatica*) (24.5%), with some white fir (*Abies alba*) (2.6%), sycamore maples (*Acer psudoplatanus*) (1.2%), and mountain ash (*Sorbus*

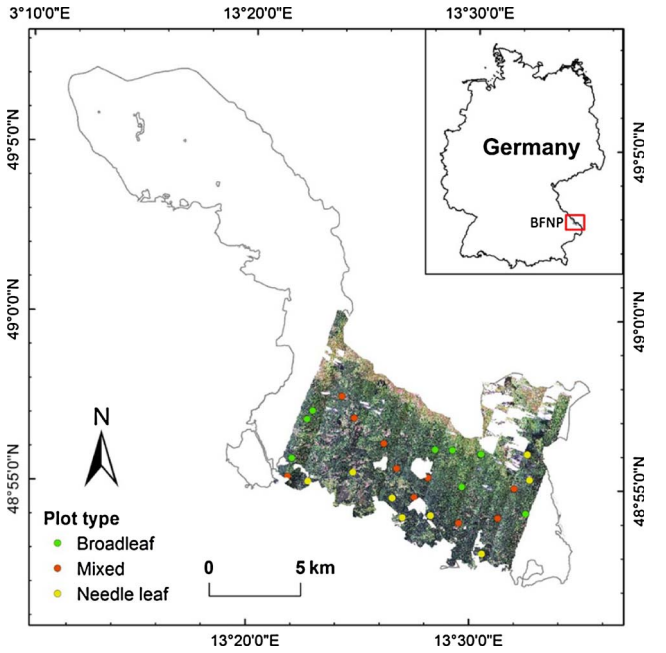

Fig. 1. Location of the study area in the Bavarian Forest National Park, Germany, and the distribution of sample plots with the HySpex image in the background.

aucuparia) (3.1%) (Heurich et al., 2010).

2.1.2. Field sampling

Fieldwork was carried out from mid-July to mid-August, 2013, using a stratified random sampling strategy. The study area was stratified into broadleaf, needle leaf, and mixed forest areas based on the land cover data obtained from the Department of Conservation and Research, Bavarian Forest National Park. The mixed forest includes both broadleaf and needle leaf species, but the fractions vary across different areas. We randomly selected 26 plots over the three vegetation types, yielding 8 broadleaf, 8 needle leaf and 10 mixed forest plots. Each plot was 30 m × 30 m in size, and a Leica GPS 1200 (Leica Geosystems AG, Heerbrugg, Switzerland) was used to record the center location of each plot (to an accuracy of approximately 1 m). Within each plot, depending on the species composition, one to three trees of each dominant overstory species were selected for leaf sampling, resulting in overall 53 broadleaf samples (44 European beech, 4 sycamore maples, 3 mountain ash, 1 goat willow (*Salix caprea*)) and 84 conifer needle samples (28 trees × 3 ages). The conifer needle samples were obtained from 21 Norway spruce and 7 white fir trees, and the shoots of needles were divided into three age classes: current growing season (C), the previous growing season (C+) and those older than the previous growing season (C++).

Sunlit leaves were collected by shooting small branches from the top canopy of each selected tree with a crossbow. Leaf samples were stored in zip-lock plastic bags with wet paper towels, and placed in a cooler before transportation to the laboratory for further measurement. The leaf mass per area (LMA, g/cm^2), leaf water content (g/cm^2, also known as equivalent water thickness (EWT, cm)) and leaf nitrogen concentration (% dry weight) were determined in the laboratory. Leaf nitrogen content (N_{area}, g/cm^2) was calculated as the product of leaf nitrogen concentration and LMA. More details regarding the sampling and laboratory analysis can be found in Wang et al. (2015b).

2.1.3. Measurements of canopy structural parameters

A number of canopy structural parameters were collected within each plot, including leaf area index (LAI), stem density, canopy closure, crown diameter and stand height. Digital hemispherical photography (DHP) and LAI-2000 (LI-COR Inc., NE, USA) are two commonly used methods for measuring LAI. DHP was used in this study because it was sometimes difficult to find open reference area for LAI-2000 in forest. LAI for each plot was calculated from five upward-pointing hemispherical photographs collected from the plot center as well as 10 m away from the center point in each diagonal direction. The images were acquired using a Canon 5D equipped with a fisheye lens leveled on a tripod at breast height (1.3 m above the ground) near dawn or dusk. Two-corner classification was applied on the images obtained, and a combined Lang and Xiang clumping correction and needle-to-shoot area ratio (Leverenz and Hinckley, 1990) was used to estimate the LAI as outlined by Woodgate et al. (2015), Macfarlane (2011), and Leblanc et al. (2005), respectively.

Stem density was calculated as the number of trees per hectare based on the number of trees in each plot. Crown closure was measured by averaging five observations within each plot using a spherical crown densiometer (Forestry Suppliers, Inc., Jackson, USA). Crown diameter was calculated from the mean of the measurements in two directions. The stand height was measured using a Nikon Forestry 550 laser rangefinder. Both crown diameter and stand height were obtained by averaging the values of five randomly selected trees in each plot. Table 1 presents the summary statistics of the field leaf and canopy parameters measured.

2.1.4. Calculation of plot-level leaf and canopy nitrogen content

Within each plot, the stand height, the diameter at breast height (DBH), and the number of trees from each dominant species were used to calculate the species fraction of foliar biomass using published allometric equations (Gower et al., 1993; Widlowski et al., 2003). The plot-level mean leaf nitrogen content (NIT_{plot}, g/cm^2, per leaf area) was calculated as the mean leaf nitrogen content for each species, weighted by the species leaf area fraction as in Eq. (1) (Homolova et al., 2013)

$$NIT_{plot} = \sum_{i=1}^{k} n_i fLAI_i \quad (1)$$

where n_i represents the average leaf nitrogen content of species i within a plot, $fLAI_i$ is the leaf area fraction of species i (in g/g), and k is the number of tree species within a plot.

The species leaf area fraction was calculated by the species foliar biomass fraction and specific leaf area (SLA, cm^2/g, the inverse ratio of LMA) as in Eq. (2) (Martin et al., 2008)

$$fLAI_i = \frac{fBiomass_i\, SLA_i}{\sum_{i=1}^{k} fBiomass_i\, SLA_i} \quad (2)$$

where $fBiomass_i$ is the foliar biomass fraction of species *i*, and SLA_i is the average specific leaf area for species *i* within a plot. The canopy nitrogen content (g/m^2, gram per ground area) was calculated by the product of LAI and plot-level mean leaf nitrogen content.

Table 1
Summary statistics of the leaf parameters and canopy parameters measured in the field (for 137 leaf samples and 26 sampling plots).

Parameter	Abbreviation	Unit	Minimum value	Maximum value	Mean
(1) Leaf parameters					
Equivalent water thickness	EWT	cm	0.0063	0.0337	0.017
Leaf mass per area	LMA	g/cm^2	0.0034	0.0291	0.014
Leaf nitrogen content	N_{area}	g/cm^2	1.43e-04	3.68e-04	2.78e-04
(2) Canopy parameters					
Leaf area index	LAI	m^2/m^2	2.85	5.14	3.61
Stem density	SD	ha^{-1}	222	1722	771
Stand height	H	m	8	38	23
Crown diameter	CD	m	1.65	15.45	5.4
Canopy closure	CC	%	77	91	82

2.1.5. Spectral measurements for sample leaves and forest background

The leaf directional-hemispherical reflectance and transmittance over the optical domain from 400 nm to 2500 nm were measured using an ASD FieldSpec-4 Pro FR spectrometer coupled with an ASD RTS-3ZC Integrating Sphere designed for the spectrometer (Analytical Spectral Devices, Inc., Boulder, CO, USA). The leaf spectral measurements of the broadleaf samples are detailed in Wang et al. (2015b). The spectral measurements of conifer needle samples were carried out according to the Daughtry's approach (Daughtry et al., 1989) which was later revised by Mesarch et al. (1999). More details can be found in Mesarch et al. (1999), Malenovský et al. (2006) and Ali et al. (2016b). In total, the leaf reflectance and transmittance of 53 broadleaf samples and 84 conifer samples were collected.

The background spectra were measured using an ASD FieldSpec-4 Pro spectrometer (Analytical Spectral devices, Inc., Boulder, CO, USA) coupled to a high density contact probe. No bare soil was found in the sampling plots, so the spectra from the background elements, such as bark, stem, dried leaves, understory and moss, were collected from a variety of representative plots.

2.2. Airborne hyperspectral data collection and processing

The hyperspectral data was obtained with a HySpex sensor through the German Aerospace Center (DLR) for the study area on 22 July 2013.

The HySpex sensor-system consists of two imaging spectrometers with spectral ranges of 400–1000 nm (visible and near infrared, VNIR) and 1000–2500 nm (short-wave infrared), which record the solar radiance reflected from the Earth's surface. The HySpex sensor comprises 160 spectral channels and 256 channels, with spectral resolutions of 3.7 and 6 nm, and spatial resolutions of 1.65 m and 3.3 m, for VNIR and SWIR, respectively. The HySpex data were recorded between 9:00 and 11:00 a.m., at an average flying height of 3000 m above ground level. The data were collected in 19 image strips for the study area with overlaps of about 30% and each strip covering about 1.1 × 11 km. The flight line was run in an almost N–S direction. Most of the image strips were acquired in clear weather conditions and none of the sample plots in the strips were covered by clouds.

The image strips were preprocessed by DLR in the following steps: (1) the digital numbers (DNs) of raw images were calibrated to at-sensor radiance; (2) ortho-rectification was performed using differential global positioning system GPS (DGPS) data and digital elevation model (DEM) data; (3) atmospheric correction was performed to convert at-sensor radiance to surface reflectance using the ATCOR4 (Atmospheric & Topographic Correction). More details can be found in Wang et al. (2016). The image reflectance values for each field plot were extracted from the preprocessed strips. A 17 × 17 pixel window (i.e. 27.2 × 27.2 m) centered on the center point of each plot was used to collect the spectra in VNIR from a sampling plot, while a 9 × 9 pixel window (i.e. 28.8 × 28.8 m) was selected for SWIR. For each window, the average spectrum to represent a plot was calculated. In total, 26 spectra were extracted over the 800–2500 nm, in which spectral region leaf nitrogen contributed most to spectra. The spectra over the 800–2500 nm were used in the following analysis because the PROSPECT-5 was recalibrated over this region (see Section 2.3.1).

The HySpex image strips were first resampled to a spatial resolution of 30 m and then mosaicked to a single image. A forest mask was applied to the image to extract the forest areas and a forest map was derived from recently updated land cover data provided by the Bavarian Forest National Park.

2.3. Model description, parameterization and inversion

2.3.1. Leaf optical properties model: PROSPECT

The PROSPECT leaf optical properties model was developed to simulate the leaf directional-hemispherical reflectance and transmittance over the optical domain from 400–2500 nm (Jacquemoud and Baret, 1990). The model only requires a few input parameters, including leaf structure parameter (N_{struc}), leaf chlorophyll content (C_{ab}, μg/cm^2), equivalent water thickness (EWT, cm) and leaf mass per area (LMA, g/cm^2). The model was improved and recalibrated by Feret et al. (2008), resulting in the new versions PROSPECT-4 and PROSPECT-5 (http://teledetection.ipgp.jussieu.fr/prosail/). PROSPECT-5 is the same as PROSPECT-4 except for the separation of total leaf chlorophyll and total leaf carotenoids (C_{cx}, μg/cm^2) in the visible range of 400–750 nm. Recently, PROSPECT-5 was used to estimate protein (C_p, g/cm^2) and cellulose + lignin content (C_{cl}, g/cm^2) in fresh leaves by simulating their effects on leaf reflectance and transmittance (Wang et al., 2015a). The recalibration of PROSPECT-5 was performed over the 800–2500 nm because protein and cellulose + lignin absorb solar radiation mostly within this range (Curran, 1989; Baret and Fourty, 1997; Feret et al., 2008). The revised PROSPECT-5 model considers N_{struc}, Cab, C_{cx}, EWT, C_p, and C_{cl} as input parameters, please see Wang et al. (2015a) for more details.

PROSPECT was originally developed for broadleaf species (Jacquemoud and Baret, 1990) and it indeed performed well with broadleaf (deciduous) trees (Feret et al., 2008; Jacquemoud et al., 1996; Jacquemoud et al., 2009; Wang et al., 2015b). Previous studies also proved that the model provided a reasonable description of needle optical properties (Ali et al., 2016b; Hernandez-Clemente et al., 2014; Jacquemoud et al., 2009; Laurent et al., 2011; Moorthy et al., 2008; Zarco-Tejada et al., 2004). The revised PROSPECT-5 described by Wang et al. (2015a) was based on broadleaf species found in the publicly available LOPEX dataset (Hosgood et al., 1995), although its applicability to conifer species was not tested due to the lack of a proper dataset.

Prior to canopy level analysis, the recalibrated PROSPECT-5 was tested for its ability to retrieve leaf nitrogen using measured fresh leaf reflectance and transmittance and then the estimation was compared with field measurements. The leaf-level analysis was performed on our dataset as well as on the publicly available LOPEX dataset. The LOPEX dataset includes more than 50 plant species, and is the most extensive dataset used for calibrating the specific absorption coefficients of protein and cellulose + lignin (Jacquemoud et al., 1996; Wang et al., 2015a). The model inversion procedure was conducted according to Wang et al. (2015a).

2.3.2. The protein-nitrogen conversion factor

Protein is calculated as 6.25 times of nitrogen in food and animal feed materials (Barton, 1987; AOAC, 1990; Jacquemoud, et al. 1996). The approach is based on the assumption that nitrogen mainly exists as amino acids in proteins, since early research found that proteins of animal origin contained approximately 16% nitrogen (Aurand et al., 1987; AOAC, 1990; Sikorski, 2001). In the LOPEX dataset, protein was determined from nitrogen with a conversion factor of 6.25 based on Kjeldahl method. This dataset has been used in a number of previous studies for the retrieval of protein using empirical approaches (Jacquemoud et al., 1995, Fourty et al., 1996; Fourty and Baret, 1998) and radiative transfer models (Jacquemoud et al., 1996; Botha et al., 2006; Wang et al., 2015a).

However, this factor may not be fully valid for plant tissues due to the existence of non-protein nitrogeneous compounds (Milton and Dintzis, 1981; Handley et al., 1989). A previous study was conducted on 90 plants species and suggested a protein-nitrogen conversion factor of 4.43 for plants (Yeoh and Wee et al., 1994). For statistical studies, using a conversion factor of 6.25 or 4.43 would change the coefficients of the models, but the values of protein may be easily converted and compared. For radiative transfer models (Jacquemoud et al., 1996; Botha et al., 2006; Wang et al., 2015a), the difference in the conversion factor would affect the magnitude of the specific absorption coefficient of protein.

Therefore, we used a conversion factor of 4.43 suggested by Yeoh and Wee et al. (1994) to calculate protein from nitrogen, and recalibrated the specific absorption coefficient of protein following the approach in Wang et al. (2015a). This newly calibrated specific absorption coefficient of protein was then used in this study.

2.3.3. Canopy reflectance model: the invertible forest reflectance model (INFORM)

The invertible forest reflectance model (INFORM) was developed to simulate the bi-directional reflectance in forest stands by combining the forest light interaction model (FLIM) (Rosema et al., 1992), scattering by arbitrary inclined leaves (SAILH) model, and PROSPECT model. INFORM is one of the hybrid models which provides a trade-off between detailed characterization of the canopy structure and model invertibility. The INFORM model accounts for the 1-dimensional, turbid medium radiative-transfer within the crowns and the 3-dimensional effects, such as crown-created shadows, the hotspot and the clumping of leaves in crowns (Schlerf and Atzberger, 2006, 2012). The model is an invertible model and has been used for estimating biophysical and biochemical forest parameters such as LAI, fAPAR, specific leaf area, and leaf dry matter content in both broadleaf and conifer stands (Schlerf and Atzberger, 2006, 2012; Yang et al., 2011). However, it has not yet been used for retrieving leaf nitrogen.

The previous submodel of PROSPECT built into INFORM was updated by the revised PROSPECT-5 to estimate protein, described in Section 2.3.1.

Table 2
The input parameters and their ranges used for generating the look-up table, using forward models in the INFORM.

Parameter	Abbreviation	Unit	Minimum value	Maximum value
Leaf structure parameter	N_{struc}	–	1.5	1.5
Leaf chlorophyll content	C_{ab}	µg/cm^2	40	40
Leaf carotenoids content	C_{cx}	µg/cm^2	10	10
Equivalent water thickness	EWT	cm	0.0063	0.0337
Leaf protein content	C_p	g/cm^2	0.0006	0.0018
Leaf cellulose + lignin content	C_{cl}	g/cm^2	0.0025	0.027
Single-tree leaf area index	LAI_s	m^2/m^2	2	8
Understory leaf area index	LAI_u	m^2/m^2	0.1	0.1
Average leaf inclination angle	ALA	degree	40	60
Stem density	SD	ha^{-1}	200	1800
Stand height	H	m	8	38
Crown diameter	CD	m	3	11
Sun zenith angle	t_s	degree	28.7	38.7
Observation zenith angle	t_o	degree	0	0
Azimuth angle	ψ	degree	126.3	182
Fraction of diffuse radiation	Skyl	–	0.1	0.1

2.3.4. Model parameterization

The range of input parameters and their fixed values are listed in Table 2.

For the revised PROSPECT-5, leaf chlorophyll and carotenoids content were held constant since these two parameters have negligible effects on leaf spectra for wavelengths longer than 800 nm. Leaf structure parameter has a small influence on canopy reflectance (Jacquemoud, 1993; Xiao et al., 2014), thus this was fixed at 1.5 based on previous studies (Ali et al., 2016b,c). Leaf nitrogen content was retrieved from laboratory measurements and the leaf protein content was calculated as 4.43 times of leaf nitrogen content (Yeoh and Wee et al., 1994). The range of leaf water and protein content were determined from field measurements. Leaf cellulose + lignin content varied from 0.00034 to 0.027 based on the range of the difference between leaf mass per area and leaf protein content (by assuming that the leaf dry mass is composed of protein and cellulose + lignin).

The range of the INFORM input parameters, including stem density, crown diameter and stand height, were set based on prior information from the field (Table 2). Single-tree LAI was calculated as the ratio of LAI and canopy closure as demonstrated in Schlerf and Atzberger (2006), which ranged from 2.5 to 8. The range of average leaf inclination angle (ALA) was set according to Ali et al. (2016c). The understory LAI was fixed at 0.1. The ratio of diffuse to total incident radiation (Skyl) was set to 0.1, as suggested in the literature (Darvishzadeh et al., 2008; Schlerf and Atzberger, 2006). The range of measurement geometry, including zenith angle of solar (t_s), observation zenith angle (t_o), and relative azimuth angle (ψ) were acquired from the HySpex image acquisition campaign. The HySpex observation zenith angle was 0, the sun zenith angle ranged from 28.7 to 38.7 based on the flight time period, and the azimuth angle varied from 126.3 to 182.

Table 3
Selected spectral subsets for model inversion to estimate leaf and canopy nitrogen content.

Spectral subset	Wavelengths (nm)
1	800–2500
2	800–1350, 1550–1750, 2000–2400
3	1550–1800, 2100–2300
4	1020, 1510, 1730, 1980, 2060, 2130, 2180, 2240, 2300

Table 4
Correlations between plot-level leaf nitrogen and other LUT parameters.

	Nitrogen	EWT	LMA	LAI	Stand density	Crown diameter
Nitrogen						
EWT	0.821**					
LMA	0.876**	0.979**				
LAI	0.451*	0.734**	0.634**			
Stand density	0.058	0.044	0.014	0.317		
Crown diameter	0.078	0.074	0.102	−0.192	−0.709**	

* Correlations significant at $p < 0.05$.
** Correlations significant at $p < 0.01$.

We used the average reflectance spectrum that was measured for understory and forest floor in representative plots (see Section 2.1.5) as a fixed background reflectance in the model.

2.3.5. Global sensitivity analysis

Sensitivity analysis helps to identify the contribution of variation in input parameters to the variability in the output canopy reflectance. There are two types of sensitivity analysis, i.e., local sensitivity analysis (LSA) and global sensitivity analysis (GSA). LSA provides information on how the variation of each input parameter individually explains the variation in the model output and ignores the interactions between model parameters, while GSA provides information of how the variation of each input parameter individually, and their interactions with each other, account for the variation of model output (Asner, 1998; Saltelli, 1999). GSA includes the simultaneous variations of model parameters (Bowyer and Danson, 2004), we therefore adopted a GSA in this study. The GSA was performed for INFORM using the ranges of input parameters presented in Table 2. A Matlab software tool (GSAT) (Cannavó, 2012) was applied to perform the GSA; see Wang et al. (2015a) for more details.

2.3.6. The look-up table inversion

There are a number of inversion approaches, such as iterative optimization, look-up table (LUT), and neural network (Kimes et al., 2000). The look-up table (LUT) inversion approach was chosen in this study, since it is a conceptually simple technique, can be easily implemented, and yields similar results to the alternatives (Combal et al., 2002; Pragnere et al., 1999). Also the LUT inversion provides a guarantee to find a global minimum, as well as the ability to apply ecological constraints during the inversion procedure (Combal et al., 2002;

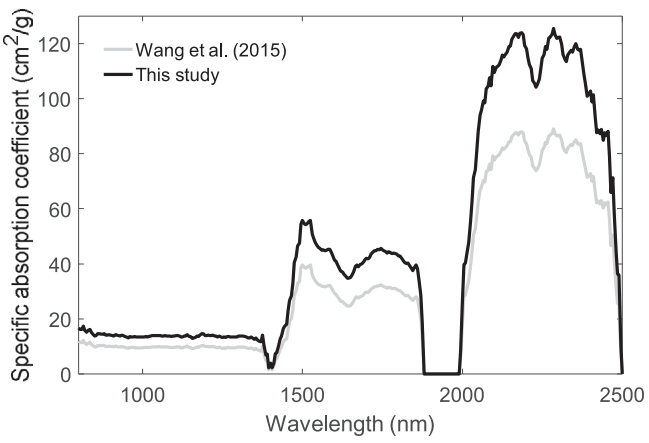

Fig. 2. Comparison of the recalibrated specific absorption coefficients of protein determined on fresh leaves using the LOPEX dataset. A conversion factor of 4.43 was used for calculating protein from nitrogen in this study. A factor of 6.25 was used in Wang et al. (2015a).

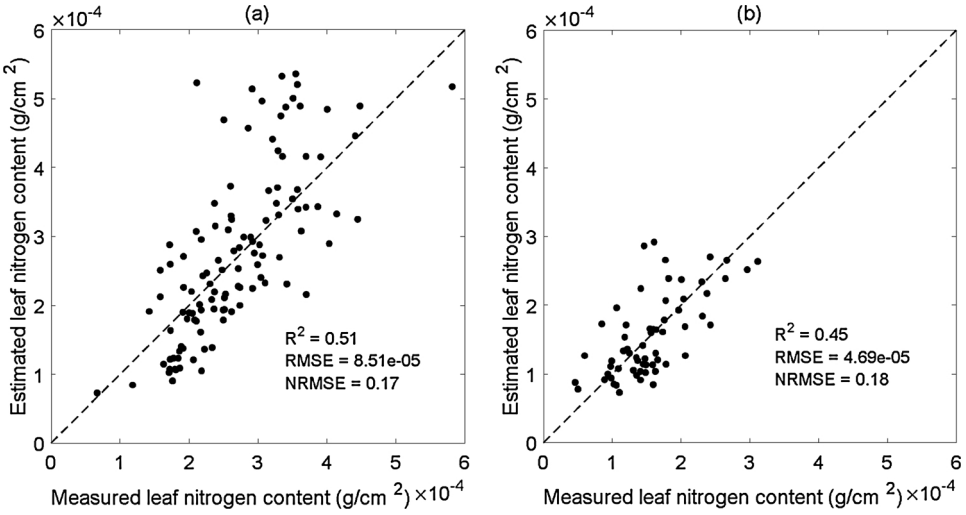

Fig. 3. Measured versus estimated leaf nitrogen content from fresh leaf spectra using the revised PROSPECT-5 inversion: (a) our dataset and (b) the LOPEX dataset.

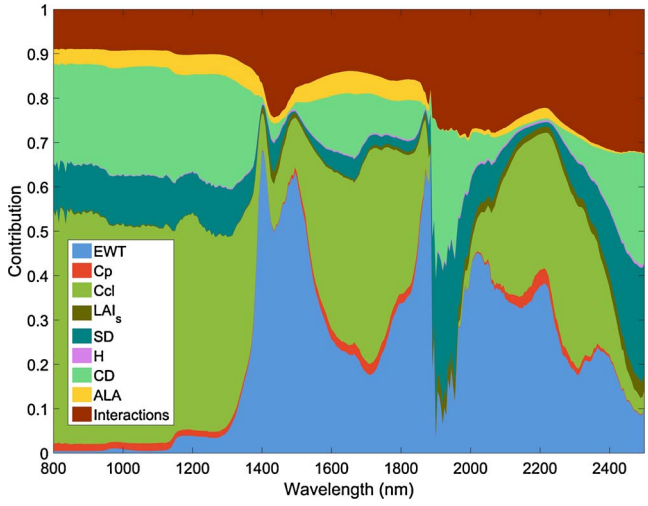

Fig. 4. Results of FAST first-order sensitivity coefficients and interactions to canopy reflectance for the global sensitivity analysis with INFORM. The abbreviations in the legend are equivalent water thickness (EWT), leaf protein content (C_p), leaf cellulose + lignin content (C_{cl}), single-tree leaf area index (LAI_s), stem density (SD), stand height (H), crown diameter (CD), and the average leaf inclination angle (ALA).

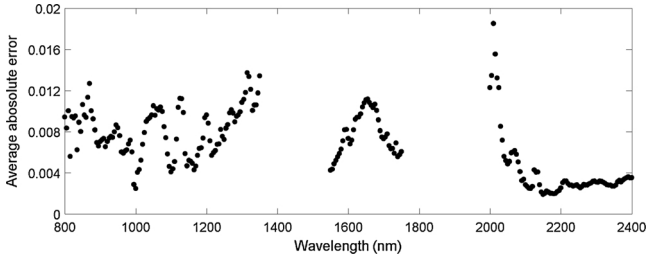

Fig. 5. The average absolute error (AAE) between measured and best-fit reflectance spectra as a function of wavelengths. The AAE has been calculated from the 26 measured canopy spectra against the best fitting look-up table (LUT) spectra for spectral subset 2 from INFORM.

Houborg et al., 2009; Jurdao et al., 2013; Yebra et al., 2008).

Prior to inversion, a LUT was built via forward modeling using different combinations of input parameters covering their prescribed range of variation (Table 2). A sufficiently large LUT is needed to ensure high accuracy for the estimated parameters, as suggested by (Darvishzadeh et al., 2008). In this study, 200,000 parameter combinations (uniform distributions) were randomly generated from the forward modeling of INFORM. To reduce unrealistic combinations of input parameters in the look-up table, we applied three ecological rules obtained from field measurements to filter out some of the simulations. The first filter selected the cases with canopy closure between 0.1 and 0.95, because values beyond this range were rarely found in our study area. The second filter utilized the empirical relationship between LAI and equivalent water thickness (LAI = 106.43*EWT + 2.57, $R^2 = 0.64$, $p < 0.001$). The third filter utilized the empirical relationship between crown diameter and stand density (CD = −0.0023*SD + 7.19, $R^2 = 0.50$, $p < 0.001$). For the latter two filters, the cases that exceeded 10% of the range derived from the maximum or minimum residue of the regression fitting were excluded. The threshold of 10% was suggested in Yebra et al. (2008). In total, four look-up tables were built for the model inversion: (1) LUT 1, with 200,000 parameter combinations; (2) LUT 2, with 95,279 selected records by applying the first filter to LUT 1; (3) LUT 3, with 70,714 selected records by applying the first and second filters to LUT 1; and (4) LUT 4, with 29,467 selected records by applying all the three filters to LUT 1.

Then, a set of parameters was identified by searching for the best fit between measured spectra and the modeled spectra of the LUT by minimizing the

$$\mathrm{RMSE} = \sqrt{\frac{\sum_{i=1}^{n} (R_{mes}(\lambda) - R_{LUT}(\lambda))^2}{n}} \quad (3)$$

where $R_{mes}(\lambda)$ is the measured reflectance at wavelength λ, $R_{LUT}(\lambda)$ is the reflectance modeled by INFORM and stored in the LUT at wavelength λ, and n is the number of wavelengths. To overcome the ill-posed problem, previous studies suggested using the mean or median of the parameters corresponding to the first 100 best matches instead of those from the best fit (Darvishzadeh et al., 2008; Schlerf and Atzberger, 2012). Therefore, 100 best matched spectra were identified, and the mean of their 100 sets of corresponding parameters were calculated as the estimates of the targeted parameters.

Previous studies have demonstrated that the use of spectral subsets rather than the full wavelengths could provide equally or more accurate estimations through model inversion (Darvishzadeh et al., 2011; Darvishzadeh et al., 2008; Wang et al., 2015a; Weiss et al., 2000). Extra bands may add some noise instead of adding useful information on

Table 5
The R^2, RMSE, NRMSE and NSE between measured and estimated leaf nitrogen content obtained using inversion of INFORM and four different look-up tables.

Spectral sampling set	Statistical parameter	LUT 1				LUT 2				LUT 3				LUT 4			
		R^2	RMSE	NRMSE	NSE	R^2	RMSE	NRMSE	NSE	R^2	RMSE	NRMSE	NSE	R^2	RMSE	NRMSE	NSE
Subset 1	Mean of 10	0.08	5.72e-05	0.29	−0.26	0.12	5.17e-05	0.26	−0.03	0.11	5.27e-05	0.27	−0.07	0.13	4.95e-05	0.25	0.06
	Mean of 20	0.06	5.73e-05	0.29	−0.26	0.18	4.74e-05	0.24	0.13	0.12	4.94e-05	0.25	0.06	0.10	4.99e-05	0.25	0.04
	Mean of 100	0.04	5.18e-05	0.26	−0.04	0.22	4.52e-05	0.23	0.21	0.28	4.39e-05	0.22	0.26	0.35	4.35e-05	0.22	0.27
Subset 2	Mean of 10	0.00	6.45e-05	0.33	−0.61	0.14	4.90e-05	0.25	0.07	0.13	4.94e-05	0.25	0.06	0.15	4.91e-05	0.25	0.07
	Mean of 20	0.00	6.36e-05	0.32	−0.56	0.20	4.74e-05	0.24	0.13	0.16	4.85e-05	0.25	0.09	0.14	4.80e-05	0.24	0.11
	Mean of 100	0.00	5.60e-05	0.28	−0.21	0.28	4.37e-05	0.22	0.26	0.33	4.28e-05	0.22	0.29	0.23	4.55e-05	0.23	0.20
Subset 3	Mean of 10	0.30	4.32e-05	0.22	0.28	0.32	4.23e-05	0.21	0.31	0.27	4.41e-05	0.22	0.25	0.28	4.42e-05	0.22	0.25
	Mean of 20	0.30	4.32e-05	0.22	0.28	0.29	4.32e-05	0.22	0.28	0.33	4.19e-05	0.21	0.32	0.34	4.22e-05	0.21	0.31
	Mean of 100	**0.31**	**4.28e-05**	**0.22**	**0.29**	0.31	4.29e-05	0.22	0.29	0.32	4.28e-05	0.22	0.29	0.30	4.35e-05	0.22	0.27
Subset 4	Mean of 10	0.00	6.74e-05	0.34	−0.75	0.25	4.92e-05	0.25	0.07	0.29	4.78e-05	0.24	0.12	0.25	4.97e-05	0.25	0.05
	Mean of 20	0.00	6.47e-05	0.33	−0.61	0.27	4.59e-05	0.23	0.19	0.34	4.44e-05	0.23	0.24	0.37	4.09e-05	0.21	0.36
	Mean of 100	0.13	5.24e-05	0.27	−0.06	**0.43**	**3.86e-05**	**0.20**	**0.43**	**0.46**	**3.79e-05**	**0.19**	**0.45**	**0.40**	**4.04e-05**	**0.20**	**0.37**

Table 6
The R^2, RMSE, NRMSE and NSE between measured and most accurately estimated leaf nitrogen content, LAI and canopy nitrogen content obtained using inversion of INFORM for broadleaf, needle leaf and mixed plots.

Category	Number of plots	Leaf nitrogen content				LAI				Canopy nitrogen content			
		R^2	RMSE	NRMSE	NSI	R^2	RMSE	NRMSE	NSI	R^2	RMSE	NRMSE	NSI
Broadleaf plots	8	0.31	4.87e-05	0.32	0.09	0.06	0.35	0.89	−5.83	0.05	2.05	0.51	−1.15
Needle leaf plots	8	0.16	2.81e-05	0.32	−0.21	0.40	0.48	0.31	0.14	0.40	1.74	0.35	0.15
Mixed plots	10	0.34	3.49e-05	0.25	0.10	0.35	0.45	0.28	0.35	0.47	1.90	0.22	0.38
Pooled plots	26	0.46	3.79e-05	0.19	0.45	0.63	0.43	0.19	0.57	0.64	1.90	0.18	0.62

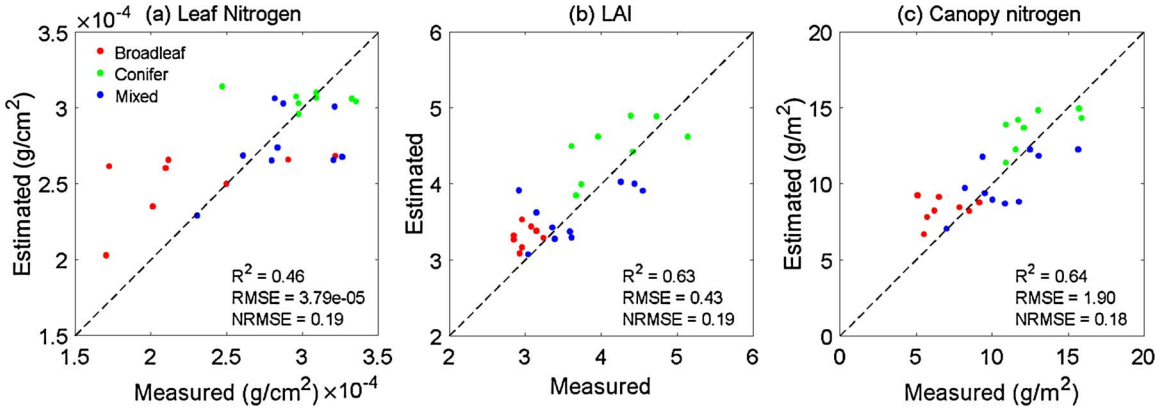

Fig. 6. Measured versus estimated parameters: (a) leaf nitrogen content (g/cm^2) (b) LAI, and (c) canopy nitrogen content (g/m^2) from measured spectra by INFORM inversion.

model inversion, which is due to the model uncertainties at certain wavelengths as well as the uncertainties in measurements (Weiss et al., 2000). We therefore performed the inversion over the following spectral subsets presented in Table 3: (1) full available wavelength range; (2) the spectral regions excluding water absorption bands; (3) the spectral regions where protein contributed relatively more to reflectance according to the global sensitivity analysis; and (4) protein absorption wavelengths based on the literature (Curran, 1989; Fourty et al., 1996).

2.4. Validation

For both leaf and canopy level analysis, the leaf nitrogen content was calculated as the estimated leaf protein content divided by 4.43. There are a number of indicators for evaluating model performance. The coefficient of determination (R^2), the root mean square error (RMSE), and the normalized RMSE (NRMSE = RMSE/range), and Nash–Sutcliffe efficiency index (NSE) were adopted in this study as suggested in Richter et al. (2012). At the leaf level, the accuracy of the retrieved leaf nitrogen content from fresh leaf reflectance and transmittance via revised PROSPECT-5 was evaluated. At the canopy level, the accuracy of the retrieved leaf nitrogen content, LAI and canopy nitrogen content from airborne hyperspectral imagery via INFORM inversion was also evaluated.

3. Results

3.1. Characteristics of leaf and canopy parameters

Table 1 gives the statistical characteristics of leaf and canopy parameters of the 26 sampling plots. The leaf nitrogen content varied from 1.43e-04 to 3.68e-04 g/cm^2, with a mean of 2.78e-04 g/cm^2. The mean LAI of all plots was 3.61, with a minimum value of 2.85 and a maximum value of 5.14. The mean stem density, tree height, crown diameter and canopy closure of the sampling plots were 771 ha^{-1}, 23 m, 5.4 m, and 82%, respectively.

Table 4 shows the Pearson correlation coefficients of the leaf and canopy parameters in the INFORM model. The plot-level leaf nitrogen content significantly correlated with LMA and EWT (r = 0.876 and 0.821, respectively, $p < 0.01$), which have been demonstrated in previous leaf level studies (Sullivan et al., 2012; Wang et al., 2015b). EWT correlated significantly with LMA and LAI (r = 0.979 and 0.734, respectively, $p < 0.01$). The stand density correlated with crown diameter (r = 0.709, $p < 0.01$).

3.2. Validation of estimated leaf nitrogen content from fresh leaf spectra

The comparison of the newly calibrated specific absorption coefficient in this study and that in Wang et al. (2015a) are shown in Fig. 2. It shows that the absorption peaks in both coefficients are consistent, but the magnitudes differ. The newly recalibrated SAC in this study is higher than that in Wang et al. (2015a). This is due to the use of the factor 4.43 to convert nitrogen to protein, which is lower than using a factor of 6.25 in Wang et al. (2015a).

Fig. 3 illustrates that leaf nitrogen content can be estimated from fresh leaf spectra using the recalibrated PROSPECT-5. The R^2, RMSE, NRMSE for our dataset were 0.51, 8.51e-05 and 0.17, respectively. The R^2, RMSE, NRMSE for LOPEX dataset were 0.45, 4.69e-05 and 0.18, respectively. This demonstrated the applicability of the recalibrated PROSPECT-5 for estimating leaf nitrogen content at the leaf level.

3.3. Global sensitivity analysis

Fig. 4 shows the FAST first-order sensitivity coefficients of the input parameters to canopy reflectance for a global sensitivity analysis with INFORM model. Cellulose + lignin contributed to canopy reflectance (around 50%) in the near infrared spectral region of 800–1300 nm, followed by crown diameter (20%) and stem density (10%). For wavelengths longer than 1300 nm, water dominated the canopy reflectance, contributing up to 60% of the explained variance. Cellulose + lignin contributed most to canopy reflectance over the spectral intervals 1500–1850 nm and 2100–2300 nm. Stem density and crown diameter had pronounced effects on canopy reflectance in the spectral intervals of 1850–2150 nm and 2300–2500 nm. In comparison, single-tree LAI, the average leaf inclination angle, and stand height had less influence on canopy reflectance over the interval 800–2500 nm. Protein had a small but noticeable impact on canopy reflectance (around 2–4%) in the spectral regions dominated by water absorption.

3.4. Validation of estimated leaf and canopy nitrogen content using INFORM inversion

Table 5 details the validation of leaf nitrogen content estimated from four look-up tables using INFORM. Leaf nitrogen content was poorly estimated from LUT 1 with no ecological constraints, and the most accurate estimates were obtained by spectral subset 3 using the mean of the best 100 cases (R^2 = 0.31, RMSE = 4.28e-05, NRMSE = 0.22, NSE = 0.29). The accuracy of estimated leaf nitrogen content was greatly improved when using LUT 2, and the most accurate estimates were provided by spectral subset 4 and the mean of the best 100 cases (R^2 = 0.43, RMSE = 3.86e-05, NRMSE = 0.20, NSE = 0.43).

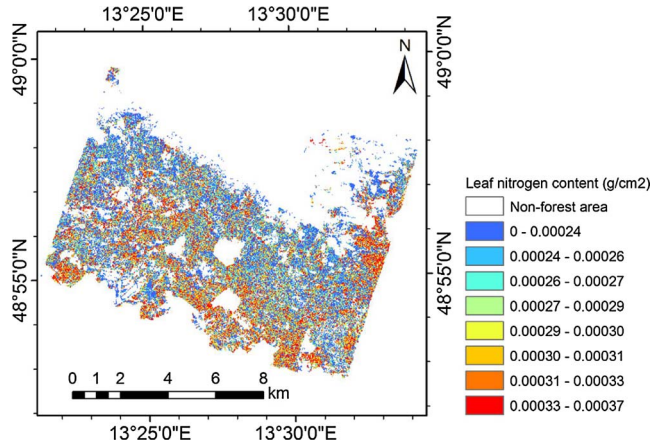

Fig. 7. Leaf nitrogen content (g/cm^2) map, generated by inversion of the INFORM model using HySpex airborne image data from 22 July 2013 in the Bavarian Forest National Park, Germany.

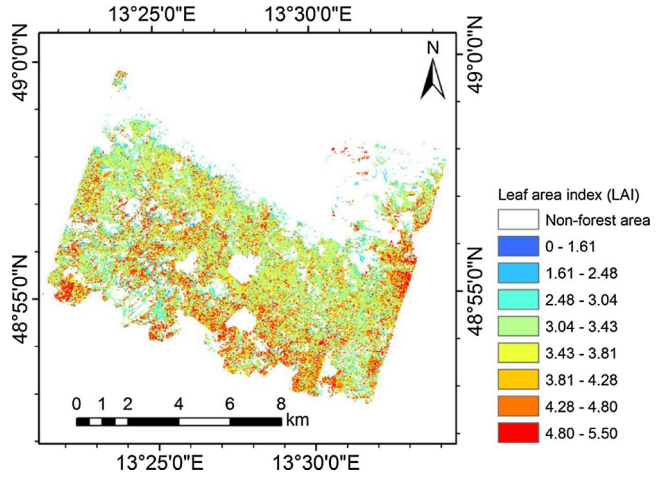

Fig. 8. LAI map, generated by inversion of the INFORM model using HySpex airborne image data from 22 July 2013 in the Bavarian Forest National Park, Germany.

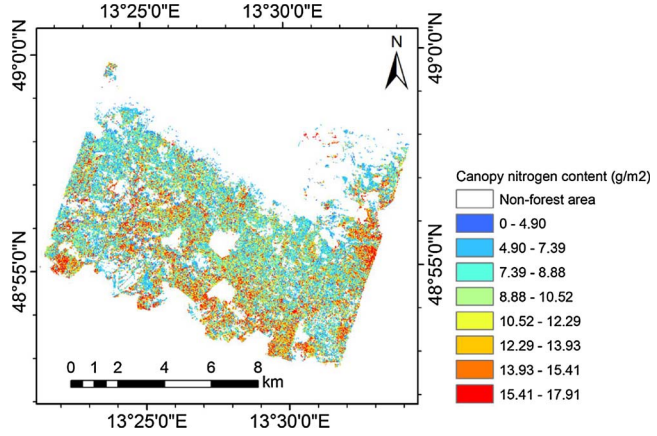

Fig. 9. Canopy nitrogen content (g/m^2) map, calculated as the product of leaf nitrogen content and LAI estimated by inversion of the INFORM model using HySpex airborne image data from 22 July 2013 in the Bavarian Forest National Park, Germany.

Compared with using LUT 2, there was a small improvement in the nitrogen estimates from the LUT 3 (R^2 = 0.46, RMSE = 3.79e-05, NRMSE = 0.19, NSE = 0.45). LUT 4 did not improve the nitrogen estimation accuracy (R^2 = 0.40, RMSE = 4.04e-05, NRMSE = 0.20, NSE = 0.20) compared with LUT 2. Accurate estimation of canopy reflectance was obtained through parameterization of the models, as demonstrated by the low average absolute error (AAE) (Darvishzadeh et al., 2008) between measured and best-fit reflectance spectra for subset 2 (AAE < 0.02, Fig. 5).

Table 6 and Fig. 6 present the validation of the most accurately estimated leaf nitrogen content, LAI and canopy nitrogen content using INFORM. Leaf nitrogen content was estimated by subset 3 and the mean of the best 100 cases found in LUT 3. LAI is a critical parameter to scale up leaf nitrogen content to canopy nitrogen content. LAI was poorly estimated by LUT 1, LUT 2 and LUT 3 (results not shown), and was moderately retrieved using LUT 4. The most accurate estimates of LAI were generated by subset 3 and the mean of the best 20 cases found in LUT 4. Canopy nitrogen content was calculated as the product of the leaf nitrogen content and LAI. Canopy nitrogen content was retrieved at a higher accuracy (R^2 = 0.64, RMSE = 1.90, NRMSE = 0.18, NSE = 0.63) than leaf nitrogen content (R^2 = 0.46, RMSE = 3.79e-05, NRMSE = 0.19, NSE = 0.45), which can be mainly attributed to the higher accuracy of the LAI estimation (R^2 = 0.63, RMSE = 0.43, NRMSE = 0.19, NSE = 0.47). However, less accurate estimates were obtained for each of the three forest types than pooled plots (Table 6).

3.5. Mapping of leaf and canopy nitrogen content from airborne hyperspectral imagery

The HySpex image, masked for forested areas (see Section 2.2), was used as input to the INFORM inversion, resulting in a map of leaf nitrogen content (Fig. 7).

LAI is a critical forest structural parameter used to scale up the leaf-level biochemical parameters to canopy level. LAI cannot be directly obtained by inversion of INFORM, but is calculated as the product of retrieved single-tree LAI and canopy closure; canopy closure was calculated using the retrieved stem density and crown diameter (Schlerf and Atzberger, 2006). Canopy nitrogen content per unit ground surface area is defined as the product of leaf nitrogen content per unit leaf area and LAI. Canopy nitrogen content was mapped (Fig. 9) based on the INFORM leaf nitrogen content map (Fig. 7) and LAI map (Fig. 8). The spatial variation of leaf nitrogen content in the generated map corresponds well with the distribution of broadleaf, needle leaf and mixed forest observed during the fieldwork. Fig. 10 details the zoomed area of estimated leaf nitrogen content, LAI and canopy nitrogen content over one of the sampling plots. As shown from the RGB image (Fig. 10(a)), this mixed forest plot included both broadleaf (in the upper left) and needle leaf stands (near the center).

4. Discussion

Prediction of leaf biochemistry at the canopy level faces a number of challenges, such as the confounding factors of canopy structure, illumination/viewing geometry and background (Asner, 1998; Yoder and Pettigrew-Crosby, 1995; Zarco-Tejada et al., 2001). Previous studies have demonstrated that lower accuracies were obtained for leaf biochemistry compared with canopy biochemistry (Darvishzadeh et al., 2008; Liang et al., 2016; Omari et al., 2013; Si et al., 2012). In these studies, an R^2 of 0.14–0.40 was obtained for leaf chlorophyll and an R^2 of 0.60–0.80 for canopy chlorophyll in grasslands and trembling aspen forest when coupled leaf-canopy radiative transfer models were

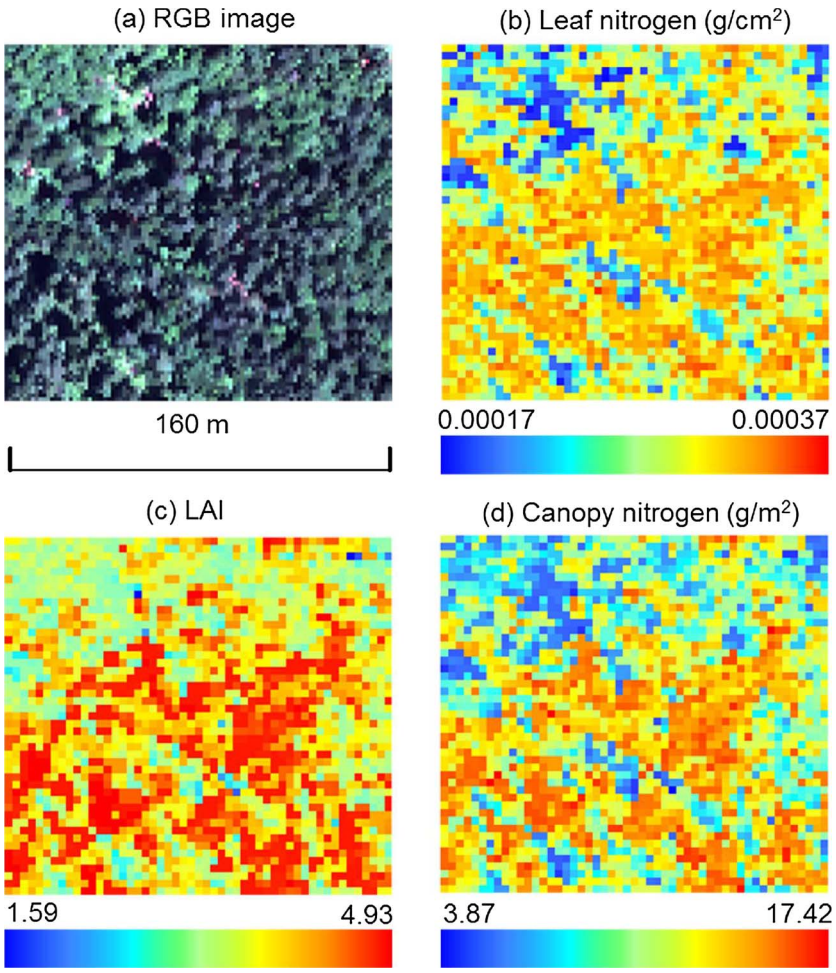

Fig. 10. Zoomed area of estimated leaf nitrogen content (g/cm^2), LAI and canopy nitrogen content (g/m^2) with one of the sampling plots in the center. The spatial resolution of the maps is 3.2 m.

inverted. Another study reported an R^2 of 0.47 for retrieved leaf chlorophyll from the canopy spectra for black spruce forest (Zhang et al., 2008). Asner et al. (2015) suggested that a validation of relative RMSE of 0.25 or less indicates good estimates, and Richter et al., (2012) also suggested good estimates with relative RMSE below 0.20 and NSE higher than 0.50. Our results showed that canopy nitrogen content can be estimated at a higher accuracy (R^2 = 0.64, NRMSE = 0.18, NSE = 0.63) than the leaf nitrogen content (R^2 = 0.46, NRMSE = 0.19, NSE = 0.45) (Table 6). The estimation accuracy of canopy nitrogen content is comparable with previous empirical studies (Martin et al., 2008; Asner et al., 2015; Wang et al., 2016). It should be noted that the spectral wavelengths from 400–799 nm were not incorporated in this study, since protein and cellulose + lignin absorption features are more prominent within the 800–2500 nm spectral region (Curran, 1989; Baret and Fourty, 1997; Feret et al., 2008). The existing correlation between nitrogen and chlorophyll may imply a higher accuracy for nitrogen estimation if red-edge region (680–780 nm) information is included.

Despite the above confounding factors, our results confirmed the feasibility of retrieving leaf nitrogen content at the canopy level by coupling a leaf radiative transfer model PROSPECT-5 and a canopy reflectance model INFORM. In previous studies, which focused on empirical models, an increased predictability of leaf biochemistry was observed when up-scaling to the canopy level (Asner and Martin, 2008; Asner et al., 2011). One reason for the feasibility of estimating leaf nitrogen content at the canopy level is the strong, multiple scattering effects in forests, which can enhance the leaf biochemical signals by up to a factor of two, especially in the near and short wave infrared regions (Baret et al., 1994). In other words, due to the relatively high LAI, the light scattering and absorption enhances the spectroscopic difference among canopies and, hence, leaf biochemistry retrieval (Asner and Martin, 2008). The second explanation is that the parameterization of the INFORM model is probably quite realistic. The INFORM model includes parameters for characterizing the canopy geometrical structure, and incorporates the forest light interaction model (FLIM) model to account for 3-dimensional effects such as shadows, the hotspot, and clumping of leaves in crowns (Schlerf and Atzberger, 2006, 2012). These enable the disassociation of the remotely sensed signal from canopy structural effects and leaf biochemical properties.

Both the direct and indirect effects of nitrogen exerting on the canopy reflectance are critical for nitrogen estimation (Lepine et al., 2016; Wang et al., 2017). The direct effect of nitrogen means that the variation in reflectance can be caused by the nitrogen absorption in leaves. This can be confirmed by the fact that protein contributed 2–4 % to the variation of canopy reflectance according to the global sensitivity analysis (Fig. 4), although that contribution was far less than that of other parameters such as water, cellulose + lignin and canopy structural properties. Also, the spectral subset 4 (including the nitrogen absorption bands) provided the most accurate estimation of nitrogen (Table 5), which suggested that the nitrogen absorption features might be detectable through the radiative transfer model. Meanwhile, the indirect effects of nitrogen on canopy reflectance should be noted due to the associations between nitrogen and other variables in this study area. First of all, the variation in canopy reflectance is partly driven by canopy structure rather than leaf nitrogen (Knyazikhin et al., 2013). Thus, there are distinct differences in the mean canopy reflectance of

broadleaf, needle leaf and mixed forest (Singh et al., 2015; Wang et al., 2017). The leaf nitrogen content also correlates well with the forest type (Ollinger et al., 2008; Knyazikhin et al., 2013; Singh et al., 2015). For example, the broadleaf (deciduous) plots with lower nitrogen had higher canopy reflectance, the needle leaf (conifer) plots with higher nitrogen had lower canopy reflectance, and mixed forest plots presented intermediate values (Ollinger et al., 2008; Lepine et al., 2016). Therefore, the estimation of nitrogen was probably due to that the INFORM model captured the difference in canopy reflectance caused by canopy structure across forest types. Secondly, leaf nitrogen is highly correlated with EWT and LMA, as observed in previous studies (Sullivan et al., 2012; Homolova et al., 2013; Wang et al., 2015b; Singh et al., 2015; Chadwick and Asner, 2016). The covariance of nitrogen with EWT might be another reason for the estimation of nitrogen, since EWT can be generally estimated with good accuracy (R^2 = 0.70–0.92, results not shown).

From Fig. 6 and Table 6, we observed that the estimation accuracy of leaf nitrogen was lower for each forest functional type than for the pooled plots, which have been shown in a number of previous studies (Dahlin et al., 2013; Lepine et al., 2016; Gokkaya et al., 2015; Singh et al., 2015; Loozen et al., 2017). The limited number of plots for each forest type (8–10) may make the indicators of model performance unsuitable for comparison. An analysis of variance showed that the functional type explained most variance (95%) in the plot-level leaf nitrogen content. The poor estimation for each forest type may be due to the limited variation within each forest type. A larger dataset of each forest type is needed to further investigate this result.

Global sensitivity analysis showed that leaf water contributed most to the variation of canopy reflectance, which is consistent with previous studies (Jacquemoud et al., 2009; Xiao et al., 2014). Leaf cellulose + lignin exerted a great influence on canopy reflectance, particularly in the NIR spectral regions (800–1300 nm). This indicated that the impact of the leaf constituents associated with internal leaf structure is transferred to the canopy level. In terms of the canopy structural parameters, we found that stand density and crown diameter were the dominant factors affecting canopy reflectance, while less influence was found from single-tree LAI and the average leaf inclination angle. This is in agreement with a recent study on the effects of canopy structural parameters on retrieving specific leaf area and leaf dry matter content from remotely sensed data (Ali et al., 2016c). In the INFORM model, canopy LAI is correlated to single-tree LAI, stem density and crown diameter, with the contribution of canopy LAI being mostly compensated by stem density and crown diameter. Therefore, a larger influence of canopy LAI on canopy reflectance is expected if single-tree LAI is converted to canopy LAI through stem density and crown diameter. Leaf protein had a small but noticeable effect on the variation of canopy reflectance (e.g. 800–1300 nm, 1600–1800 nm, 2100–2300 nm) as simulated using INFORM.

RTMs are inherently constrained by the ill-posed inverse problem (Combal et al., 2002). In other words, firstly, different combinations of input parameter may generate similar spectra. Secondly, measurement and model uncertainties will lead to inconsistencies during model inversion. Regularization techniques have been proposed to minimize the ill-posed inverse problem, such as using prior information (Combal et al., 2002), spectral subsets (Darvishzadeh et al., 2008; Wang et al., 2015a; Weiss et al., 2000), ecological constraints (Jurdao et al., 2013; Yebra and Chuvieco, 2009), and a spatial regularization approach (Houborg et al., 2009; Houborg et al., 2015).

In this study, we used the prior information from field measurements, which constrains the input parameters and avoids unrealistic solutions. Ecological rules were applied to the look-up table to reduce unrealistic combinations of input parameters. Instead of adopting the best case LUT, the mean of the first 100 best cases was selected as the solution. The latter provided more robust results for the retrieved parameters (Table 5). The spectral subset 4 generated the most accurate estimations, followed by subset 3 (Table 5). Subset 4 includes the nitrogen absorption bands while subset 3 is the spectral region that protein contributed most to the canopy reflectance. This demonstrates the physical mechanisms of nitrogen estimation. Due to the masking effect of water, water removal techniques will be required to enhance the nitrogen absorption features in further research (Wang et al., 2015a), such as integration with continuum removal (Clark and Roush, 1984; Malenovský et al., 2006) as well as with wavelet transforms (Banskota et al., 2013).

The application of ecological constraints improved the estimation accuracy, and if further refined may improve the transferability of RTM models to other species and sites. The first filter, of canopy closure between 0.1 and 0.95, largely improved the estimation accuracy, and can be applied to most forest areas. The second ecological rule utilized the negative relationship between stand density and canopy diameter, which may be applied to closed forest like the study area here but would not work for open forest. The third filter was built on the empirical relationship between EWT and LAI, which did not improve the estimation accuracy of nitrogen but improved the estimation of LAI. This can be attributed to the good estimates of EWT (R^2 = 0.70–0.92, results not shown). The essence of RTM models may result in less accurate estimation when compared with empirical approaches. A compromise between retrieval accuracy and model transferability needs to be sought when applying regulation techniques to model inversion. RTM models improve the understanding of physical mechanisms in nitrogen estimation, and empirical approaches laid the foundation of developing RTM models. The RTM models and empirical approaches are not exclusive, and their combination would complement each other when retrieving leaf and canopy nitrogen (Wang, 2016). Furthermore, hybrid methods are recommended for the retrieval of vegetation variables, which combine the generalization of RTMs with the flexibility and computational efficiency of non-parametric regression methods (Verrelst et al., 2015).

Fig. 7 demonstrated that the spatial pattern of leaf nitrogen content and that of structural and biochemical characteristics of broad- and needle-leaf forest stand, due to the covariance of nitrogen and other variables in this study area. The areas with higher nitrogen content are in good agreement with the distribution of needle leaf forest, which is mainly found in the southern valley areas, while low nitrogen areas are consistent with the broadleaf forest located in the north at a higher elevation. This was also confirmed by our observations during the fieldwork (Wang et al., 2015b). We calculated the mean and standard deviation of leaf nitrogen content for all image pixels in the forest area. The mean and standard deviation of INFORM leaf nitrogen were 2.7e-04 g/cm^2 and 6.8e-05, respectively, which is close to values of sampled plots measured in the field (2.8e-04 g/cm^2 and 5.2e-05). The canopy nitrogen content per unit ground surface area ranged from 4.90 to 18.91 g/m^2 for forest pixels (Fig. 9). The canopy nitrogen map highly correlated with both the leaf nitrogen map and the LAI map. The variance of canopy nitrogen across different plant functional types is being driven almost equally by the values of leaf nitrogen and LAI.

5. Conclusions

We have evaluated the feasibility of combining leaf and canopy radiative transfer models to retrieve leaf and canopy nitrogen content using airborne hyperspectral measurements. Leaf protein had a small but noticeable effect on the canopy reflectance. The look-up table detailed the canopy information and viewing geometry, which enabled the separation of canopy structural effects from leaf optical properties. Canopy nitrogen content was retrieved at a higher accuracy than leaf nitrogen content, which can be attributed to having good estimates of LAI. Inversion techniques, such as using prior information, ecological constraints, spectral subsets, and statistical parameters of a certain number of best solutions further improved our estimation accuracy. The most accurate estimation of leaf nitrogen was obtained when using spectral subset 4 and the mean of the first 100 cases. The estimation of

nitrogen could be explained by both the direct and indirect effects of nitrogen on the variations in canopy reflectance. To fully understand the physical mechanisms for nitrogen estimation using radiative transfer models, a more extensive dataset is needed. The leaf nitrogen and canopy nitrogen maps were generated by applying the inversion procedure to the whole hyperspectral imagery, and the spatial variation corresponded well with the distribution of plant functional types.

The robustness and transferability of radiative transfer models suggests that the approaches proposed in this study may be transferred to other sites with different natural and environmental conditions. Ancillary information and ecological rules for new sites would be necessary to obtain an accurate estimation. With the aid of light detection and ranging (LiDar), canopy structural parameters that are inputs to the canopy model can be obtained and used as constraints in the model inversion (Asner et al., 2015; Combal et al., 2002; Gokkaya et al., 2015; Niemann et al., 2012). Hybrid methods of coupling radiative transfer models with empirical approaches through machine learning regression algorithms are needed for accurate retrieval of nitrogen (Verrelst et al., 2015; Wang, 2016). Larger scale maps of foliar nitrogen could be generated for modeling ecosystems and assessing biodiversity if hyperspectral satellites such as EnMAP (Guanter et al., 2015) and HyspIRI ((NRC) 2007) become operational.

Acknowledgments

Zhihui Wang was supported by the China Scholarship Council (grant 201204910232) and co-funded by the ITC Research Fund (grant 93003032) of the Faculty of Geo-Information Science and Earth Observation (ITC), University of Twente, the Netherlands. We are grateful to the “Applied spectroscopy” team of the German Aerospace Center (DLR) and the Bavarian Forest National Park for assistance with fieldwork. We acknowledge support by the “Data Pool Forestry” data-sharing initiative of the Bavarian Forest National Park. We would like to thank Abebe M. Ali for the assistance in the fieldwork. We thank Jackie Senior for editing the manuscript and the anonymous reviewers for their valuable comments.

References

Ali, A.M., Skidmore, A.K., Darvishzadeh, R., Duren, Iv., Holzwarth, S., Müller, J., 2016a. Retrieval of forest leaf functional traits from HySpex imagery using radiative transfer models and continuous wavelet analysis. ISPRS J. Photogramm. Remote Sens. 122, 68–80.

Ali, A.M., Darvishzadeh, R., Skidmore, A.K., Duren, Iv., Heiden, U., Heurich, M., 2016b. Estimating leaf functional traits by inversion of PROSPECT: assessing leaf dry matter content and specific leaf area in mixed mountainous forest. Int. J. Appl. Earth Obs. Geoinf. 45 (Part A), 66–76.

Ali, A.M., Darvishzadeh, R., Skidmore, A.K., Duren, Iv., 2016c. Effects of canopy structural variables on retrieval of leaf dry matter content and specific leaf area from remotely sensed data. IEEE J. Sel. Top. Appl. Earth Obs. Remote Sens. 9, 898–909.

AOAC, 1990. Official Methods of Analysis. Association of Official Analytical Chemists, Arlington, VA, USA.

Asner, G.P., 1998. Biophysical and biochemical sources of variability in canopy reflectance. Remote Sens. Environ. 64, 234–253.

Asner, G.P., Martin, R.E., 2008. Spectral and chemical analysis of tropical forests: scaling from leaf to canopy levels. Remote Sens. Environ. 112, 3958–3970.

Asner, G.P., Martin, R.E., Anderson, C.B., Knapp, D.E., 2015. Quantifying forest canopy traits: imaging spectroscopy versus field survey. Remote Sens. Environ. 158, 15–27.

Asner, G.P., Martin, R.E., Knapp, D.E., Tupayachi, R., Anderson, C., Carranza, L., et al., 2011. Spectroscopy of canopy chemicals in humid tropical forests. Remote Sens. Environ. 115, 3587–3598.

Atzberger, C., 2000.). Development of an Invertible Forest Reflectance Model: The INFOR-Model.

Aurand, L.W., Woods, A.E., Wells, M.R., 1987. Food Composition and Analysis. Van Nostrand Reinhold, New York.

Axelsson, C., Skidmore, A.K., Schlerf, M., Fauzi, A., Verhoef, W., 2013. Hyperspectral analysis of mangrove foliar chemistry using PLSR and support vector regression. Int. J. Remote Sens. 34, 1724–1743.

Banskota, A., Wynne, R.H., Thomas, V.A., Serbin, S.P., Kayastha, N., Gastellu-Etchegorry, J.P., et al., 2013. Investigating the utility of wavelet transforms for inverting a 3-D radiative transfer model using hyperspectral data to retrieve forest LAI. Remote Sens. 5, 2639–2659.

Baret, F., Fourty, T., 1997. Estimation of leaf water content and specific leaf weight from reflectance and transmittance measurements. Agronomie 17 (9–10), 455–464.

Baret, F., Vanderbilt, V.C., Steven, M.D., Jacquemoud, S., 1994. Use of spectral analogy to evaluate canopy reflectance sensitivity to leaf optical properties. Remote Sens. Environ. 48, 253–260.

Barton, F.E., 1987. Analytical Application to Fibrous Foods and Commodities. American Association of Cereal Chemists, St. Paul, MN.

Botha, E.J., Zebarth, B.J., Leblon, B., 2006. Non-destructive estimation of potato leaf chlorophyll and protein contents from hyperspectral measurements using the PROSPECT radiative transfer model. Can. J. Plant Sci. 86, 279–291.

Bowyer, P., Danson, F.M., 2004. Sensitivity of spectral reflectance to variation in live fuel moisture content at leaf and canopy level. Remote Sens. Environ. 92, 297–308.

Cannavó, F., 2012. Sensitivity analysis for volcanic source modeling quality assessment and model selection. Comput. Geosci. 44, 52–59.

Chadwick, K.D., Asner, G.P., 2016. Organismic-scale remote sensing of canopy foliar traits in lowland tropical forests. Remote Sens. 8, 87.

Cho, M.A., 2007. Hyperspectral Remote Sensing of Biochemical and Biophysical Parameters: The Derivate Red-Edge" Double-Peak Feature", A Nuisance or an Opportunity? pp. 206. University of Twente Faculty of Geo-Information and Earth Observation (ITC), Enschede, the Netherlands.

Clark, R.N., Roush, T.L., 1984. Reflectance spectroscopy: quantitative analysis techniques for remote sensing applications. J. Geophys. Res.: Solid Earth 89, 6329–6340.

Combal, B., Baret, F., Weiss, M., Trubuil, A., Mace, D., Pragnere, A., et al., 2002. Retrieval of canopy biophysical variables from bidirectional reflectance – using prior information to solve the ill-posed inverse problem. Remote Sens. Environ. 84, 1–15.

Coops, N.C., Smith, M.L., Martin, M.E., Ollinger, S.V., 2003. Prediction of eucalypt foliage nitrogen content from satellite-derived hyperspectral data. IEEE Trans. Geosci. Remote Sens. 41, 1338–1346.

Curran, P.J., 1989. Remote sensing of foliar chemistry. Remote Sens. Environ. 30, 271–278.

Curran, P.J., Dungan, J.L., Peterson, D.L., 2001. Estimating the foliar biochemical concentration of leaves with reflectance spectrometry testing the Kokaly and Clark methodologies. Remote Sens. Environ. 76, 349–359.

Dahlin, K.M., Asner, G.P., Field, C.B., 2013. Environmental and community controls on plant canopy chemistry in a Mediterranean-type ecosystem. Proc. Natl. Acad. Sci. U. S. A. 110, 6895–6900.

Darvishzadeh, R., Atzberger, C., Skidmore, A., Schlerf, M., 2011. Mapping grassland leaf area index with airborne hyperspectral imagery: a comparison study of statistical approaches and inversion of radiative transfer models. ISPRS J. Photogramm. Remote Sens. 66, 894–906.

Darvishzadeh, R., Skidmore, A., Schlerf, M., Atzberger, C., 2008. Inversion of a radiative transfer model for estimating vegetation LAI and chlorophyll in a heterogeneous grassland. Remote Sens. Environ. 112, 2592–2604.

Daughtry, C.S.T., Biehl, L.L., Ranson, K.J., 1989. A new technique to measure the spectral properties of conifer needles. Remote Sens. Environ. 27, 81–91.

Elvidge, C.D., 1990. Visible and near infrared reflectance characteristics of dry plant materials. Int. J. Remote Sens. 11, 1775–1795.

Evans, J., 1989. Photosynthesis and nitrogen relationships in leaves of C3 plants. Oecologia 78, 9–19.

Evans, J.R., 1983. Nitrogen and photosynthesis in the flag leaf of wheat (Triticum aestivum L.). Plant Physiol. 72, 297–302.

Feret, J.B., Francois, C., Asner, G.P., Gitelson, A.A., Martin, R.E., Bidel, L.P.R., et al., 2008. PROSPECT-4 and 5: advances in the leaf optical properties model separating photosynthetic pigments. Remote Sens. Environ. 112, 3030–3043.

Ferwerda, J.G., Jones, S.D., 2006. Continuous wavelet transformations for hyperspectral feature detection. In: Riedl, A., Kainz, W., Elmes, G.A. (Eds.), Progress in Spatial Data Handling. Springer, Berlin, Heidelberg, pp. 167–178.

Field, C., Mooney, H.A., 1986. The photosynthesis-nitrogen relationship in wild plants. In: Givnish, T.J. (Ed.), On the Economy of Plant Form and Function. Cambridge University Press, Cambridge, pp. 25–55.

Fourty, T., Baret, F., 1998. On spectral estimates of fresh leaf biochemistry. Int. J. Remote Sens. 19, 1283–1297.

Fourty, T., Baret, F., Jacquemoud, S., Schmuck, G., Verdebout, J., 1996. Leaf optical properties with explicit description of its biochemical composition: direct and inverse problems. Remote Sens. Environ. 56, 104–117.

Gastellu-Etchegorry, J.P., Demarez, V., Pinel, V., Zagolski, F., 1996. Modeling radiative transfer in heterogeneous 3-D vegetation canopies. Remote Sens. Environ. 58, 131–156.

Gokkaya, K., Thomas, V., Noland, T.L., McCaughey, H., Morrison, I., Treitz, P., 2015. Prediction of macronutrients at the canopy level using spaceborne imaging spectroscopy and LiDAR data in a mixedwood boreal forest. Remote Sens. 7, 9045–9069.

Gower, S.T., Reich, P.B., Son, Y., 1993. Canopy dynamics and aboveground production of five tree species with different leaf longevities. Tree Physiol. 12, 327–345.

Guanter, L., Kaufmann, H., Segl, K., Foerster, S., Rogass, C., Chabrillat, S., et al., 2015. The EnMAP spaceborne imaging spectroscopy mission for earth observation. Remote Sens. 7, 8830–8857.

Handley, L.L., Mehran, M., Moore, C.A., Cooper, W.J., 1989. Nitrogen-to-protein conversion factors for two tropical C_4 grasses, *Brachiaria mutica* (Forsk) Stapf and Pennisetum purpureum Schumach. Biotropica 21, 88–90.

Hernandez-Clemente, R., Navarro-Cerrillo, R.M., Zarco-Tejada, P.J., 2014. Deriving predictive relationships of carotenoid content at the canopy level in a conifer forest using hyperspectral imagery and model simulation. IEEE Trans. Geosci. Remote Sens. 52, 5206–5217.

Heurich, M., Beudert, B., Rall, H., Křenová, Z., 2010. National parks as model regions for interdisciplinary long-term ecological research: the Bavarian Forest and Šumavá national parks underway to transboundary ecosystem research. In: Müller, F., Baessler, C., Schubert, H., Klotz, S. (Eds.), Long-Term Ecological Research. Springer, Science & Business Media, pp. 327–344.

Homolova, L., Maenovsky, Z., Clevers, J., Garcia-Santos, G., Schaeprnan, M.E., 2013. Review of optical-based remote sensing for plant trait mapping. Ecol. Complex. 15, 1–16.
Hosgood, B., Jacquemoud, S., Andreoli, G., Verdebout, J.P.G., Schmuck, G., 1995. Leaf Optical Properties Experiment 93 (LOPEX93) Report EUR-16095-EN. European Commission—Joint Research Centre, Ispra (Italy).
Houborg, R., Anderson, M., Daughtry, C., 2009. Utility of an image-based canopy reflectance modeling tool for remote estimation of LAI and leaf chlorophyll content at the field scale. Remote Sens. Environ. 113, 259–274.
Houborg, R., McCabe, M., Cescatti, A., Gao, F., Schull, M., Gitelson, A., 2015. Joint leaf chlorophyll content and leaf area index retrieval from Landsat data using a regularized model inversion system (REGFLEC). Remote Sens. Environ. 159, 203–221.
Huang, Z., Turner, B.J., Dury, S.J., Wallis, I.R., Foley, W.J., 2004. Estimating foliage nitrogen concentration from HYMAP data using continuum removal analysis. Remote Sens. Environ. 93, 18–29.
Huemmrich, K.F., 2001. The GeoSail model: a simple addition to the SAIL model to describe discontinuous canopy reflectance. Remote Sens. Environ. 75, 423–431.
Jacquemoud, S., 1993. Inversion of the PROSPECT + SAIL canopy reflectance model from AVIRIS equivalent spectra: theoretical study. Remote Sens. Environ. 44, 281–292.
Jacquemoud, S., Bacour, C., Poilve, H., Frangi, J.P., 2000. Comparison of four radiative transfer models to simulate plant canopies reflectance: direct and inverse mode. Remote Sens. Environ. 74, 471–481.
Jacquemoud, S., Baret, F., 1990. PROSPECT: a model of leaf optical properties spectra. Remote Sens. Environ. 34, 75–91.
Jacquemoud, S., Verdebout, J., Schmuck, G., Andreoli, G., Hosgood, B., 1995. Investigation of leaf biochemistry by statistics. Remote Sens. Environ. 54, 180–188.
Jacquemoud, S., Ustin, S.L., Verdebout, J., Schmuck, G., Andreoli, G., Hosgood, B., 1996. Estimating leaf biochemistry using the PROSPECT leaf optical properties model. Remote Sens. Environ. 56, 194–202.
Jacquemoud, S., Verhoef, W., Baret, F., Bacour, C., Zarco-Tejada, P.J., Asner, G.P., et al., 2009. PROSPECT plus SAIL models: a review of use for vegetation characterization. Remote Sens. Environ. 113, S56–S66.
Jurdao, S., Yebra, M., Guerschman, J.P., Chuvieco, E., 2013. Regional estimation of woodland moisture content by inverting radiative transfer models. Remote Sens. Environ. 132, 59–70.
Kimes, D.S., Knyazikhin, Y., Privette, J.L., Abuelgasim, A.A., Gao, F., 2000. Inversion methods for physically-based models. Remote Sens. Rev. 18, 381–439.
Knyazikhin, Y., Schull, M.A., Stenberg, P., Mottus, M., Rautiainen, M., Yang, Y., et al., 2013. Hyperspectral remote sensing of foliar nitrogen content. Proc. Natl. Acad. Sci. U. S. A. 110, E185–192.
Kokaly, R.F., Clark, R.N., 1999. Spectroscopic determination of leaf biochemistry using band-depth analysis of absorption features and stepwise multiple linear regression. Remote Sens. Environ. 67, 267–287.
Kokaly, R.F., Asner, G.P., Ollinger, S.V., Martin, M.E., Wessman, C.A., 2009. Characterizing canopy biochemistry from imaging spectroscopy and its application to ecosystem studies. Remote Sens. Environ. 113, S78–S91.
Lamarque, J.F., Kiehl, J.T., Brasseur, G.P., Butler, T., Cameron-Smith, P., Collins, W.D., et al., 2005. Assessing future nitrogen deposition and carbon cycle feedback using a multimodel approach: analysis of nitrogen deposition. J. Geophys. Res.-Atmos. 110, 1–21.
Laurent, V.C.E., Verhoef, W., Clevers, J., Schaepman, M.E., 2011. Inversion of a coupled canopy-atmosphere model using multi-angular top-of-atmosphere radiance data: A forest case study. Remote Sens. Environ. 115, 2603–2612.
Leblanc, S.G., Chen, J.M., Fernandes, R., Deering, D.W., Conley, A., 2005. Methodology comparison for canopy structure parameters extraction from digital hemispherical photography in boreal forests. Agric. For. Meteorol. 129, 187–207.
Lepine, L.C., Ollinger, S.V., Ouimette, A.P., Martin, M.E., 2016. Examining spectral reflectance features related to foliar nitrogen in forests: implications for broad-scale nitrogen mapping. Remote Sens. Environ. 173, 174–186.
Leverenz, J.W., Hinckley, T.M., 1990. Shoot structure, leaf area index and productivity of evergreen conifer stands. Tree Physiol. 6, 135–149.
Li, X., Strahler, A., 1985. Geometric-optical modeling of a conifer forest canopy. IEEE Trans. Geosci. Remote Sens. GE-23, 705–721.
Liang, L., Qin, Z., Zhao, S., Di, L., Zhang, C., Deng, M., et al., 2016. Estimating crop chlorophyll content with hyperspectral vegetation indices and the hybrid inversion method. Int. J. Remote Sens. 37, 2923–2949.
Loozen, Y., Rebel, K.T., Karssenberg, D., Wassen, M.J., Sardans, J., Peñuelas, J., de Jong, S.M., 2017. Regional detection of canopy nitrogen in Mediterranean forests using the spaceborne MERIS Terrestrial Chlorophyll Index. Biogeosci. Discuss 2017, 1–32. http://dx.doi.org/10.5194/bg-2017-228. (see: https://www.biogeosciences-discuss.net/bg-2017-228/).
Macfarlane, C., 2011. Classification method of mixed pixels does not affect canopy metrics from digital images of forest overstorey. Agric. For. Meteorol. 151, 833–840.
Malenovský, Z., Albrechtová, J., Lhoták ová, Z., Zurita-Milla, R., Clevers, J.G.P.W., Schaepman, M.E., Cudlín, P., 2006. Applicability of the PROSPECT model for Norway spruce needles. Int. J. Remote Sens. 27, 5315–5340.
Martin, M.E., Plourde, L.C., Ollinger, S.V., Smith, M.L., McNeil, B.E., 2008. A generalizable method for remote sensing of canopy nitrogen across a wide range of forest ecosystems. Remote Sens. Environ. 112, 3511–3519.
Mesarch, Mark A., Walter-Shea, Elizabeth A., Asner, Gregory P., Middleton, Elizabeth M., Chan, Stephen S., 1999. A revised measurement methodology for conifer needles spectral optical properties: evaluating the influence of gaps between elements. Remote Sens. Environ. 68, 177–192.
Milton, K., Dintzis, F.R., 1981. Nitrogen-to-protein conversion factors for tropical plant samples. Biotropica 177–181.
Moorthy, I., Miller, J.R., Noland, T.L., 2008. Estimating chlorophyll concentration in conifer needles with hyperspectral data: an assessment at the needle and canopy level. Remote Sens. Environ. 112, 2824–2838.
Morford, S.L., Houlton, B.Z., Dahlgren, R.A., 2011. Increased forest ecosystem carbon and nitrogen storage from nitrogen rich bedrock. Nature 477, 78–81.
Niemann, K.O., Quinn, G., Goodenough, D.G., Visintini, F., Loos, R., 2012. Addressing the effects of canopy structure on the remote sensing of foliar chemistry of a 3-dimensional, radiometrically porous surface. IEEE J. Sel. Top. Appl. Earth Obs. Remote Sens. 5, 584–593.
(NRC), N.R.C., 2007. Earth Science and Applications from Space: National Imperatives for the Next Decade and Beyond. National Academies Press, Washington, DC, USA.
Ollinger, S.V., Richardson, A.D., Martin, M.E., Hollinger, D.Y., Frolking, S.E., Reich, P.B., et al., 2008. Canopy nitrogen, carbon assimilation, and albedo in temperate and boreal forests: functional relations and potential climate feedbacks. Proc. Natl. Acad. Sci. U. S. A. 105, 19336–19341.
Omari, K., White, H.P., Staenz, K., King, D.J., 2013. Retrieval of forest canopy parameters by inversion of the PROFLAIR leaf-canopy reflectance model using the LUT approach. IEEE J. Sel. Top. Appl. Earth Obs. Remote Sens. 1–10.
Pereira, H.M., Ferrier, S., Walters, M., Geller, G.N., Jongman, R.H.G., Scholes, R.J., et al., 2013. Essential biodiversity variables. Science 339, 277–278.
Pinty, B., Widlowski, J.L., Taberner, M., Gobron, N., Verstraete, M.M., Disney, M., et al., 2004. Radiation transfer model intercomparison (RAMI) exercise: results from the second phase. J. Geophys. Res.-Atmos. 109, D06210.
Pragnere, A., Baret, F., Weiss, M., Myneni, R., Knyazikhin, Y., Wang, L.B., 1999. Comparison of three radiative transfer model inversion techniques to estimate canopy biophysical variables from remote sensing data. Geoscience and Remote Sensing Symposium, 1999. IGARSS' 99 Proceedings. IEEE 1999 International. pp. 1093–1095.
Ramoelo, A., Skidmore, A.K., Schlerf, M., Mathieu, R., Heitkönig, I.M.A., 2011. Water-removed spectra increase the retrieval accuracy when estimating savanna grass nitrogen and phosphorus concentrations. ISPRS J. Photogramm. Remote Sens. 66, 408–417.
Reich, P.B., 2012. Key canopy traits drive forest productivity. Proc. R. Soc. B: Biol. Sci. 279, 2128–2134.
Richter, K., Atzberger, C., Hank, T.B., Mauser, W., 2012. Derivation of biophysical variables from earth observation data: validation and statistical measures. J. Appl. Remote Sens. 6 063557-1.
Rosema, A., Verhoef, W., Noorbergen, H., Borgesius, J.J., 1992. A new forest light interaction model in support of forest monitoring. Remote Sens. Environ. 42, 23–41.
Saltelli, A., 1999. Sensitivity analysis: could better methods be used? J. Geophys. Res.: Atmos. 104, 3789–3793.
Schlerf, M., Atzberger, C., 2006. Inversion of a forest reflectance model to estimate structural canopy variables from hyperspectral remote sensing data. Remote Sens. Environ. 100, 281–294.
Schlerf, M., Atzberger, C., 2012. Vegetation structure retrieval in beech and spruce forests using spectrodirectional satellite data. IEEE J. Sel. Top. Appl. Earth Obs. Remote Sens. 5, 8–17.
Schlerf, M., Atzberger, C., Hill, J., Buddenbaum, H., Werner, W., Schueler, G., 2010. Retrieval of chlorophyll and nitrogen in Norway spruce (Picea abies L. Karst.) using imaging spectroscopy. Int. J. Appl. Earth Obs. Geoinf. 12, 17–26.
Serrano, L., Peñuelas, J., Ustin, S.L., 2002. Remote sensing of nitrogen and lignin in Mediterranean vegetation from AVIRIS data: decomposing biochemical from structural signals. Remote Sens. Environ. 81, 355–364.
Si, Y., Schlerf, M., Zurita-Milla, R., Skidmore, A., Wang, T., 2012. Mapping spatio-temporal variation of grassland quantity and quality using MERIS data and the PROSAIL model. Remote Sens. Environ. 121, 415–425.
Sikorski, Z.E., 2001. Chemical and Functional Properties of Food Components. CRC Press, Boca Raton.
Singh, A., Serbin, S.P., McNeil, B.E., Kingdon, C.C., Townsend, P.A., 2015. Imaging spectroscopy algorithms for mapping canopy foliar chemical and morphological traits and their uncertainties. Ecol. Appl. 25 (8), 2180–2197.
Skidmore, A.K., Ferwerda, J.G., Mutanga, O., Van Wieren, S.E., Peel, M., Grant, R.C., et al., 2010. Forage quality of savannas—simultaneously mapping foliar protein and polyphenols for trees and grass using hyperspectral imagery. Remote Sens. Environ. 114, 64–72.
Skidmore, A.K., Pettorelli, N., Coops, N.C., Geller, G.N., Hansen, M., Lucas, R., et al., 2015. Environmental science: agree on biodiversity metrics to track from space. Nature 523, 403–405.
Sullivan, F.B., Ollinger, S.V., Martin, M.E., Ducey, M.J., Lepine, L.C., Wicklein, H.F., 2012. Foliar nitrogen in relation to plant traits and reflectance properties of New Hampshire forests. Can. J. For. Res. 43, 18–27.
Verhoef, W., 1984. Light scattering by leaf layers with application to canopy reflectance modeling: the SAIL model. Remote Sens. Environ. 16, 125–141.
Verrelst, J., Camps-Valls, G., Muñoz-Marí, J., Rivera, J.P., Veroustraete, F., Clevers, J.G., Moreno, J., 2015. Optical remote sensing and the retrieval of terrestrial vegetation bio-geophysical properties–a review. ISPRS J. Photogramm. Remote Sens. 108, 273–290.
Wang, Z., Skidmore, A.K., Wang, T., Darvishzadeh, R., Hearne, J., 2015a. Applicability of the PROSPECT model for estimating protein and cellulose + lignin in fresh leaves. Remote Sens. Environ. 168, 205–218.
Wang, Z., Skidmore, A.K., Darvishzadeh, R., Heiden, U., Heurich, M., Wang, T., 2015b. Leaf nitrogen content indirectly estimated by leaf traits derived from the PROSPECT model. IEEE J. Sel. Top. Appl. Earth Obs. Remote Sens. 8, 3172–3182.
Wang, Z., Wang, T., Darvishzadeh, R., Skidmore, A., Jones, S., Suarez, L., et al., 2016. Vegetation indices for mapping canopy foliar nitrogen in a mixed temperate forest. Remote Sens. 8, 491.
Wang, Z., 2016. Mapping Spatial Variation of Foliar Nitrogen Using Hyperspectral

Remote Sensing. pp. 145,. University of Twente Faculty of Geo-Information and Earth Observation (ITC), Royal Melbourne Institute of Technology, Enschede, Melbourne.
Wang, Z., Skidmore, A.K., Wang, T., Darvishzadeh, R., Heiden, U., Heurich, M., et al., 2017. Canopy foliar nitrogen retrieved from airborne hyperspectral imagery by correcting for canopy structure effects. Int. J. Appl. Earth Obs. Geoinf. 54, 84–94.
Weiss, M., Baret, F., Myneni, R.B., Pragnère, A., Knyazikhin, Y., 2000. Investigation of a model inversion technique to estimate canopy biophysical variables from spectral and directional reflectance data. Agronomie 20, 3–22.
Widlowski, J.-L., Verstraete, M., Pinty, B., Gobron, N., 2003. Allometric Relationships of Selected European Tree Species: Parametrizations of Tree Architecture for the Purpose of 3-D Canopy Reflectance Models Used in the Interpretation of Remote Sensing: Betula pubescens, Fagus sylvatica, Larix decidua, Picea abies, Pinus sylvestris. EC Joint Research Centre, Ispra, Italy.
Woodgate, W., Jones, S.D., Suarez, L., Hill, M.J., Armston, J.D., Wilkes, P., et al., 2015. Understanding the variability in ground-based methods for retrieving canopy openness, gap fraction, and leaf area index in diverse forest systems. Agric. For. Meteorol. 205, 83–95.
Wright, I.J., Reich, P.B., Westoby, M., Ackerly, D.D., Baruch, Z., Bongers, F., et al., 2004. The worldwide leaf economics spectrum. Nature 428, 821–827.
Xiao, Y., Zhao, W., Zhou, D., Gong, H., 2014. Sensitivity analysis of vegetation reflectance to biochemical and biophysical variables at leaf, canopy, and regional scales. IEEE Trans. Geosci. Remote Sens. 52, 4014–4024.
Yang, G.J., Zhao, C.J., Liu, Q., Huang, W.J., Wang, J.H., 2011. Inversion of a radiative transfer model for estimating forest LAI from multisource and multiangular optical remote sensing data. IEEE Trans. Geosci. Remote Sens. 49, 988–1000.
Yebra, M., Chuvieco, E., 2009. Linking ecological information and radiative transfer models to estimate fuel moisture content in the Mediterranean region of Spain: solving the ill-posed inverse problem. Remote Sens. Environ. 113, 2403–2411.
Yebra, M., Chuvieco, E., Riaño, D., 2008. Estimation of live fuel moisture content from MODIS images for fire risk assessment. Agric. For. Meteorol. 148, 523–536.
Yeoh, H.H., Wee, Y.C., 1994. Leaf protein contents and nitrogen-to-protein conversion factors for 90 plant species. Food Chem. 49, 245–250.
Yoder, B.J., Pettigrew-Crosby, R.E., 1995. Predicting nitrogen and chlorophyll content and concentrations from reflectance spectra (400–2500 nm) at leaf and canopy scales. Remote Sens. Environ. 53, 199–211.
Yuan, H., Ma, R., Atzberger, C., Li, F., Loiselle, S., Luo, J., 2015. Estimating forest fAPAR from multispectral Landsat-8 data using the invertible forest reflectance model INFORM. Remote Sens. 7, 7425.
Zaehle, S., Medlyn, B.E., De Kauwe, M.G., Walker, A.P., Dietze, M.C., Hickler, T., et al., 2014. Evaluation of 11 terrestrial carbon–nitrogen cycle models against observations from two temperate Free-Air CO2 Enrichment studies. New Phytol. 202, 803–822.
Zarco-Tejada, P.J., Miller, J.R., Harron, J., Hu, B.X., Noland, T.L., Goel, N., et al., 2004. Needle chlorophyll content estimation through model inversion using hyperspectral data from boreal conifer forest canopies. Remote Sens. Environ. 89, 189–199.
Zarco-Tejada, P.J., Miller, J.R., Noland, T.L., Mohammed, G.H., Sampson, P.H., 2001. Scaling-up and model inversion methods with narrowband optical indices for chlorophyll content estimation in closed forest canopies with hyperspectral data. IEEE Trans. Geosci. Remote Sens. 39, 1491–1507.
Zhang, C., Li, C., Chen, X., Luo, G., Li, L., Li, X., et al., 2013. A spatial-explicit dynamic vegetation model that couples carbon, water, and nitrogen processes for arid and semiarid ecosystems. J. Arid Land 5, 102–117.
Zhang, Y.Q., Chen, J.M., Miller, J.R., Noland, T.L., 2008. Leaf chlorophyll content retrieval from airborne hyperspectral remote sensing imagery. Remote Sens. Environ. 112, 3234–3247.